

## Feasibility of Fast Neutron Source in Versatile Thorium Target System

Kwangho Ju <sup>a</sup> and Yonghee Kim <sup>a\*</sup>

<sup>a</sup>Department of Nuclear & Quantum Engineering, KAIST, Daejeon, Republic of Korea

\*Corresponding author: [yongheekim@kaist.ac.kr](mailto:yongheekim@kaist.ac.kr)

### 1. Introduction

Neutron sources are getting attention as an essential tool in many fields such as physics, chemistry, biology and material science. The most commonly recognized neutron source is a nuclear reactor over the last several decades despite of concerns about safety and nuclear waste disposal. Other small-scale neutron sources such as D-D, D-T, AmBe and <sup>252</sup>Cf have not been a complete alternative as their strength is not enough for various applications. In particular, an intense fast neutron source is vitally required to investigate the radiation effects of candidate materials for the use in nuclear fission and fusion systems.

Recently, advancements of accelerator technologies enable to generate intensive neutron source [1]. For example, United States and Ukraine have collaborated to design and construct a large-scale neutron source of accelerator-driven subcritical system (ADS) with 100 kW electron beam [2]. Meanwhile, in South Korea, High Flux Advanced Neutron Application Reactor (HANARO) is the only high-performance neutron source for various users with different needs [3]. Given the high cost and limited accessibility of other international neutron source facilities, more affordable fast neutron sources deserve research efforts.

In support of developing alternative fast neutron source, we perform a feasibility of versatile thorium target system using the conventional electron accelerator. In the proposed thorium target system, fast neutrons are generated by the photo-nuclear ( $\gamma, xn$ ) reactions. In this paper, the fast neutron flux ( $E > 0.821$  MeV) of the proposed neutron source is compared with that of the HANARO research reactor.

### 2. Photo-neutrons in thorium target

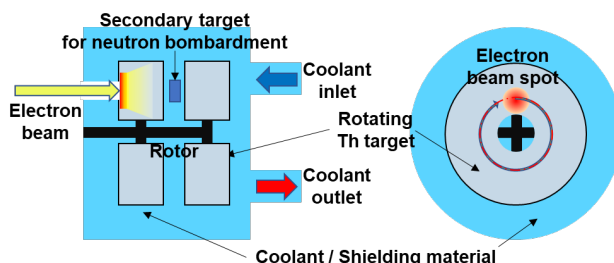


Fig. 1. Schematic diagram of versatile thorium target system.

Figure 1 illustrates a schematic diagram of the versatile thorium target system. A cylindrical thorium target is directly bombarded by an electron beam to

generate Bremsstrahlung photons and trigger ( $\gamma, xn$ ) photonuclear reactions to produce fast neutrons. There is a neutron target (secondary target in Fig.1) between splitted Th targets cladded with 0.2 mm tantalum layer. The pair of Th targets should be rotating to dissipate deposited heat while the secondary target is fixed during electron beam bombardment. This system makes it possible to bombard the fixed target with energetic neutrons from ( $\gamma, xn$ ) reactions.

In this study, a 500 kW electron beam with a 70 MeV energy and a 7.14 mA current is considered to evaluate the neutron flux of thorium target system. For a given electron beam power, the optimal electron energy is chosen based on the yield of the mother nuclei for two  $\alpha$ -emitters [4]. A neutron spectrum is estimated with TALYS-generated Evaluated Nuclear Data Libraries (TENDL) cross-sections [5]. Monte Carlo N-Particle transport (MCNP) version 6.2 code is used to simulate photonuclear reactions and secondary neutrons emitted by ( $\gamma, xn$ ) reactions in natural thorium target. In this study, the depletion of thorium-232 is neglected for one-year beam irradiation of 500 kW electron beam. Therefore, photonuclear reactions and their neutron production of only <sup>232</sup>Th are considered in MCNP6 calculation. This is acceptable as the actual depleted amount of <sup>232</sup>Th is only about 0.12 %.

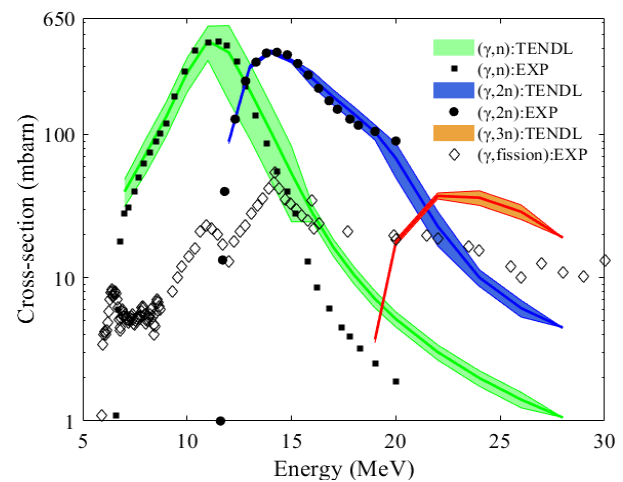


Fig. 2. Comparison between TENDL and experimental data for photon-induced reactions of <sup>232</sup>Th.

Figure 2 compares experimental cross-sections of <sup>232</sup>Th with corresponding TENDL data. Unlike <sup>232</sup>Th( $\gamma, n$ ), <sup>231</sup>Th and <sup>232</sup>Th( $\gamma, 2n$ ) <sup>230</sup>Th reactions, no experimental data of <sup>232</sup>Th( $\gamma, 3n$ ) <sup>229</sup>Th reaction have been reported. It is worthwhile to note that except for

some overrated TENDL data of  $(\gamma, n)$  cross-section at a high energy tail, most of the experimental cross-section are within one standard deviation of the TENDL data. While TALYS generally provides rather uncertain parameters for photonuclear reactions, it is known that the parameter of  $(\gamma, xn)$  reactions of heavy nuclides is rather invariant with the atomic mass number. Based on the comparison in Fig. 2 and the general credibility of the TENDL library, the  $(\gamma, xn)$  data of  $^{232}\text{Th}$  in TENDL seems to be quite acceptable.

### 3. Results

#### 3.1 Optimal position of neutron target

When the thorium target is bombarded by a 500 kW electron beam, the magnitude of neutron flux varies depending on a beam size and target's position.

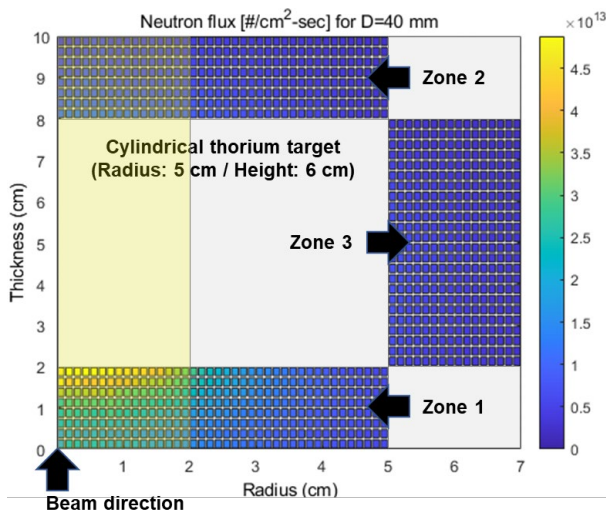


Fig. 3. Spatial distribution of neutron flux at non-target region

Figure 3 shows the spatial distribution of neutron flux at non-target region when the target is irradiated by electron beam with 40 mm diameter. For a sensitivity study, the neutron flux is tallied in the surrounding air region with small meshes, i.e., 0.125 cm and 0.250 cm in radial and axial directions, respectively.

Table 1. Maximum neutron flux at non-target region.

Beam diameter	Maximum neutron flux ( $\#/\text{cm}^2\text{-sec}$ )		
	Zone 1	Zone 2	Zone 3
15 mm	1.06E+14	1.54E+13	6.73E+12
40 mm	4.88E+13	1.19E+13	7.04E+12

Table 1 shows neutron flux at different positions for two beam diameters, either 15 mm or 40 mm. The maximum neutron flux occurs at zone 1 (irradiated surface) and minimum one at zone 3 for both beam diameters. Neutron flux at zone 3 is higher with a larger beam diameter due to higher neutron leakage through

the radial surface of the target, while the peak neutron flux noticeably lower at zone 1 and zone 2 for the 40 mm beam size. Though the neutron flux is maximized at zone 1, it is not allowed to place a neutron target ahead of the thorium target since it can act as an obstacle to the generation of Bremsstrahlung photons and photo-neutrons. It is also noteworthy that cooling of the Th target with a 500 kW electron beam is very challenging. [4]. Therefore, the Th target is splitted and neutron target is placed between the two Th targets.

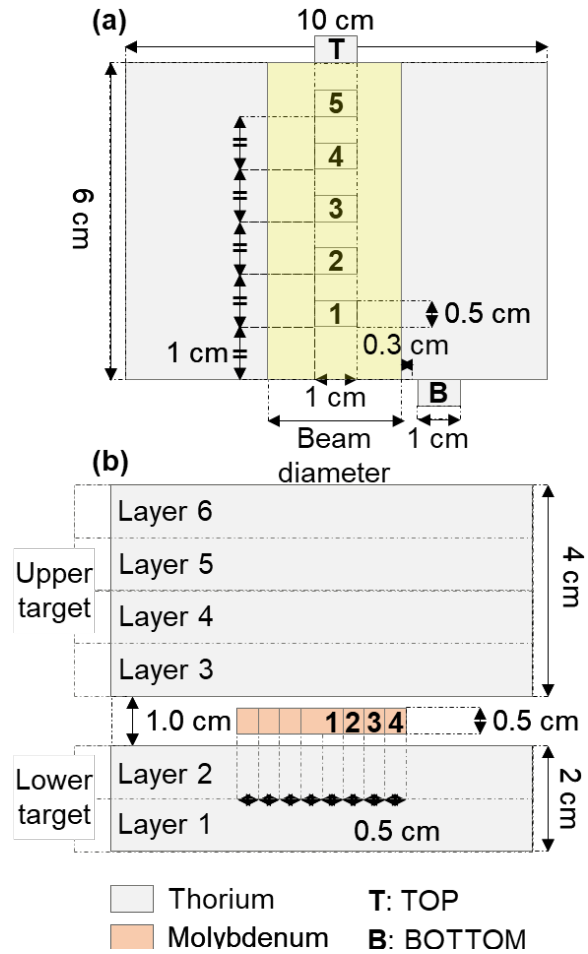


Fig. 4. Schematic diagram of thorium and molybdenum target to find out optimal position of neutron target.

In order to find out optimum position of the neutron target, first of all, the neutron flux is tallied in a small Th volume with a 1 cm diameter and a 0.5 cm height as shown in Fig. 4(a). The bottom target is placed outside of beam diameter to avoid the direct electron irradiation, while other 5 Th targets in the original thorium target and top target are on beam axis.

Table 2. Fast neutron flux ( $E > 0.8$  MeV) for the original thorium target.

Target position (Depth)	Beam diameter		
	15 mm	30 mm	40 mm
Bottom	1.26E+14	5.48E+13	3.82E+13

Zone 1 (1 cm)	1.83E+14	1.01E+14	7.11E+13
Zone 2 (2 cm)	9.81E+13	6.60E+13	4.95E+13
Zone 3 (3 cm)	5.13E+13	3.89E+13	3.18E+13
Zone 4 (4 cm)	2.66E+13	2.27E+13	1.93E+13
Zone 5 (5 cm)	1.42E+13	1.30E+13	1.14E+13
Top	6.07E+12	6.05E+12	6.02E+12

Table 2 shows fast neutron fluxes for different positions of small Th targets in Fig. 4(a). Compared with the maximum neutron flux at zone 1 in Table 1, the neutron flux of bottom target in Table 2 is lowered. This is because the target is placed far from the electron beam spot or neutron source.

In the thorium target, neutron flux is maximized at 1 cm depth and linearly decreases with a depth regardless of electron beam diameters. Taking into account the axial flux distribution and the photo-production of the  $\alpha$ -emitters in the Th target, the Th target is split into two parts as shown in Fig. 4(b). The gap between the splitted targets is temporarily set to 1 cm and a neutron target with 2 cm radius and 0.5 cm height is placed in between them. In this study, molybdenum target is chosen for neutron-induced  $^{99m}\text{Tc}$  production.

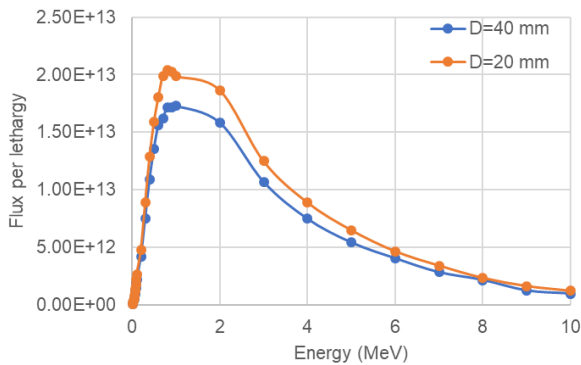


Fig. 5. Neutron spectrum with different beam diameters.

Table 3. Fast neutron flux ( $E > 0.8$  MeV) at the molybdenum target.

Radially subdivided zone in Mo target	Beam diameter	
	20 mm	40 mm
Zone 1 (0.0 – 0.5 cm)	4.61E+13	2.99E+13
Zone 2 (0.5 – 1.0 cm)	3.93E+13	2.79E+13
Zone 3 (1.0 – 1.5 cm)	2.88E+13	2.50E+13
Zone 4 (1.5 – 2.0 cm)	1.97E+13	2.00E+13
Averaged flux	2.79E+13	2.37E+13

The molybdenum target is subdivided into small zones in radial direction to see the position-dependent neutron flux in the Mo target as shown in Table 3 and detail neutron spectra are given in Fig. 5. It is clear that the fast neutron flux increases with a smaller diameter of electron beam due to a closer location of

photonuclear reactions and dense generation of fast neutrons. With an advanced cooling system that ensures sufficient a heat removal capability, the neutron flux can be enhanced further for a smaller diameter of electron beam.

Table 4. Variation of isotopic yield of mother nuclei

Yield in layer (GBq)	Original [Fig. 4(a)]		Splitted [Fig. 4(b)]		Loss (%)	
	$^{229}\text{Th}$	$^{231}\text{Pa}$	$^{229}\text{Th}$	$^{231}\text{Pa}$	$^{229}\text{Th}$	$^{231}\text{Pa}$
Layer 1	0.676	3.698	0.677	3.701	0.1	0.1
Layer 2	0.524	3.827	0.524	3.824	-0.1	-0.1
Total (Lower)	1.201	7.525	1.201	7.525	-	-
Layer 3	0.227	2.148	0.178	1.792	-21.6	-21.6
Layer 4	0.100	1.176	0.079	0.968	-21.4	-21.4
Layer 5	0.045	0.633	0.035	0.515	-21.6	-21.6
Layer 6	0.020	0.336	0.016	0.272	-22.1	-22.1
Total (Upper)	0.393	4.294	0.308	3.547	-21.6	-17.4

The variation of isotopic yield of the mother nuclei for two  $\alpha$ -emitters  $^{225}\text{Ac}$  and  $^{227}\text{Th}$  is shown in Table 4. While there is no change in the lower target, the yield decrement is clearly observed in the upper target due to the gap and neutron target. Consequently, it is clear that the  $\alpha$ -emitters yields are significantly reduced by adding the neutron target in the middle of the Th target. It is necessary to optimize the neutron target design such that the  $\alpha$ -emitters production capability should be maximized.

### 3.2 Comparison with neutron flux in HANARO.

In order to validate the feasibility of the newly proposed Th target as a neutron source, the available fast neutron flux in Table 3 is compared with a fast neutron flux in HANARO.

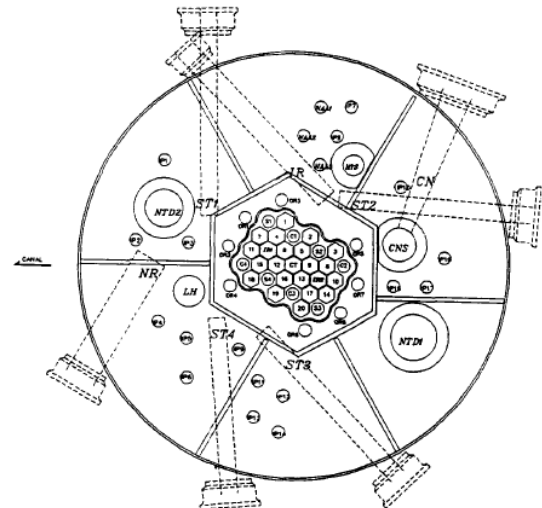


Fig. 6. Test holes and nose of beam tube configuration of HANARO.

HANARO users can choose appropriate position depending on neutron energy: CT and IR for nuclear fuel irradiation with energetic neutron; OR and IP for radioactive isotope production and burnup test with thermal and epithermal neutrons [6,7].

Table 5. Averaged neutron flux at test holes and nose of beam tubes in HANARO.

Case	Energy	Thermal (E < 0.625 eV)	Fast (E > 0.821 MeV)
	Test hole	CT	3.13E+14
IR1		2.73E+14	1.36E+14
IR2		2.81E+14	1.41E+14
OR3		2.50E+14	1.61E+13
IP15		1.60E+14	1.73E+12
Nose of beam tube	ST1	1.89E+14	1.08E+13
	ST2	2.22E+14	7.61E+12
	ST3	2.24E+14	7.35E+12
	NR	4.32E+13	1.25E+11
	CN	9.68E+13	6.10E+11

Table 5 shows the fast and thermal neutron flux at test holes and nose of beam tube in HANARO. The neutron flux in test hole is higher than that in nose of beam tube due to a shielding near a neutron target. In general, the neutron flux at nose of beam tube is more thermalized. The fast neutron flux in the new thorium target system is higher than those in the nose of beam tube at fast energy region and is comparable to those in OR and IP test holes. It is also noted that the peak fast neutron flux in the Th target is quite higher than those of OR and IP holes. Thermal neutron flux is not compared due to the minimum energy of photo-neutron is about 10 keV and there is no moderator near the neutron target.

#### 4. Conclusions and future work

A feasibility of a fast neutron source in an electron-bombarded thorium target system has been performed in this paper. The neutron flux at fast region is about  $2.37\text{E}+13/\text{cm}^2\text{-sec}$ , which is comparable to those in HANARO. The neutron flux varies with different target configuration and it is expected that much higher fast neutron flux could be achievable in the proposed Th target. Further optimization of the Th target will be done to maximize the fast neutron flux in the neutron target without compromising the yield of the precious  $\alpha$ -emitters.

#### REFERENCES

[1] *Development Opportunities for Small and Medium Scale Accelerator Driven Neutron Sources – Report*

of a technical meeting held in Vienna, 18–21 May 2004, no. 1439. Vienna: INTERNATIONAL ATOMIC ENERGY AGENCY, 2005.

[2] A. Talamo and Y. Gohar, “Medical Isotope Production Analyses In KIPT Neutron Source Facility,” Argonne National Lab.(ANL), Argonne, IL (United States), 2016.

[3] C. Choi, H. Kim, K. Lee, C. Lee, and J. Sohn, “Present situations and perspectives on the advanced utilization of HANARO,” *Phys. B Condens. Matter*, vol. 311, no. 1–2, pp. 34–39, 2002.

[4] K. Ju and Y. Kim, “Feasibility of a novel photoproduction of  $^{225}\text{Ac}$  and  $^{227}\text{Th}$  with natural thorium target,” *Sci. Rep.*, vol. 12, no. 1, pp. 1–9, 2022.

[5] A. J. Koning, D. Rochman, J.-C. Sublet, N. Dzysiuk, M. Fleming, and S. Van Der Marck, “TENDL: complete nuclear data library for innovative nuclear science and technology,” *Nucl. Data Sheets*, vol. 155, pp. 1–55, 2019.

[6] M. S. Cho *et al.*, “Development of a Device for a Material Irradiation Test in the OR Test Hole,” Korea Atomic Energy Research Institute, 2008.

[7] H. Kim, H. R. Kim, K. H. Lee, and J. B. Lee, “Design characteristics and startup tests of HANARO: The newly in-service Korean research reactor,” *J. Nucl. Sci. Technol.*, vol. 33, no. 7, pp. 527–538, 1996.